

TOWARDS A GENERAL APPROACH TO THE DEPROTONATION OF CARBON ACIDS, INCLUDING NITROALKANES

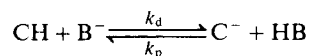
LUÍS G. ARNAUT

Departamento de Química, Universidade de Coimbra, 3049 Coimbra Codex, Portugal

The deprotonation of nitroalkanes and ketones was studied through the intersecting state model of Formosinho. The anomalous Brønsted coefficients observed when substituted nitroalkanes react with a common base are explained in terms of variable transition-state electronic structures. These are very sensitive to substitution in the nitroalkane, owing to the high electron affinity of the nitro group. In ketones, such electronic effects are much attenuated. The transition states are characterized by the bond order, n^* , which is quantitatively correlated to the field/inductive and resonance effects of the substituents. The deprotonation of fluorene and other carbon acids was also studied. The theoretical model applied shows that all these reactions follow a mechanistic continuum, dictated by the extent into which the group directly bonded to the acidic carbon is mixed in the reaction coordinate.

INTRODUCTION

Linear free energy relationships (LFER) are one of the most important tools available to physical organic chemists to probe transition state structures and relative energies. The LFER of reference in proton transfer reactions:



is the Brønsted relationship:

$$k_d = G_d(K_a)^\alpha \quad \text{or} \quad k_p = G_p(1/K_a)^\beta \quad (1)$$

where G_d and G_p are constants for a given reaction medium and temperature.

After the work of Leffler¹ and Hammond,² Brønsted coefficients have been associated with transition-state structures for series of structurally related species. More specifically, in acid catalysis α should approach the lower limit of zero for very exothermic reactions with rates controlled by diffusion, and should approach the upper limit of unity for endothermic, slow, reactions. Moreover, for all cases the condition $\alpha + \beta = 1$ should be verified.³ Despite its usefulness, the physical meaning of the Brønsted α and β coefficients has been seriously questioned. In the following, we survey evidence from the literature which shows that Brønsted coefficients are poor guides to transition-state structures. We then briefly mention some theoretical models which provide some insight into this failure, and offer alternative ways to probe the transition states. Next, an extension of the intersecting state model is

introduced, incorporating variable transition-state bond orders, and is applied quantitatively to base catalysis of carbon acid deprotonations. Finally, we present results which show that all carbon acids are amenable, without anomalies, to our theoretical treatment.

The first serious criticism of the validity of Brønsted coefficients as a guide to transition structures came from the work of Bordwell and co-workers on nitroalkanes. The deprotonation of series of substituted nitroalkanes by hydroxide ion in water exhibits anomalous Brønsted α values.⁴ According to the Leffler–Hammond postulate, in these exothermic reactions the transition state is expected to be close energetically to the reactants and α should approach zero.² However, a value of α larger than unity was obtained. In qualitative terms, the kinetic acidities of carbon acids are found to be more sensitive to substituent effects than the equilibrium acidities.⁵ This result has dramatic consequences for the application of kinetic models based on the variation of the free energy of activation as a function of a unidimensional reaction coordinate (RC), such as in current LFER. To rationalize and predict trends in reactivity, these relationships utilize the concept of series of reactions, using structurally related compounds with substituents placed sufficiently far from the reaction centre that the reactants, transition state and products have similar functional dependences on substituent perturbation. However, any representation of a series of reactions as a function of a single progress variable requires, for each reaction, two energy minima (reactants and products) separated

by a maximum (transition state). This freezes the relative positions, in a series, of the minima along the RC. Thus unidimensional models predict the change in the free energy of activation, ΔG^\ddagger , to be smaller or equal to the change in the free energy of reaction, ΔG^0 , along the series. This is implicit in the condition $\alpha < 1$. Within this formalism, a substituent that decreases ΔG^\ddagger more than ΔG^0 , requires a specific transition-state stabilization mechanism which is less important for reactants or products. Such a mechanism cannot be incorporated in LFER, where ΔG^\ddagger is a function of only one parameter.

It was known for some time that in the series CH_3NO_2 , $\text{CH}_3\text{CH}_2\text{NO}_2$, and $(\text{CH}_3)_2\text{CHNO}_2$, the acidity increase was followed by a decrease in the rates of deprotonation by hydroxide ion; experimentally, $\alpha = -0.48$. This unprecedented situation was believed to be caused by the specificity of the structural variation at the acidic carbon, namely by steric effects, and was not subject to any detailed analysis before the work of Bordwell and co-workers.^{4,6} However, we must emphasize that in the deprotonation by hydroxide ion of a series of ketones also substituted in the acidic carbon, $\text{CH}_3\text{COCH}_2\text{R}$ ($\text{R} = \text{OCH}_3$, $\text{COOCH}_2\text{CH}_3$, SO_3^- , CH_3 , $\text{CH}_3\text{CH}_2\text{COCH}_2\text{CH}_3$), we can obtain an excellent Brønsted plot (correlation coefficient $r = 0.998$) with $\alpha = 0.56$. Apparently, specific interactions are not intrinsic to acidic carbon substitution and, again, nitroalkanes behave anomalously. Steric effects with α -substituents do not occur in the deprotonation of ketones and are minimal in the replacement of a hydrogen on the carbanionic carbon derived from a nitroalkane by the rather bulky $\text{ArCH}(\text{OH})$ moiety.⁷ It is important to note that anomalous Brønsted plots are not exclusive for nitroalkanes.³ For example, proton transfers between 9-alkylfluorenes and 9-alkylfluorenyl anions in diethyl ether show Brønsted slopes ranging from 0.7 to 1.8.⁸ A good model for nitroalkanes must also shed some light into this system.

The interpretation of Brønsted plots involving nitroalkanes is further complicated as the deprotonation of a nitroalkane by a series of nitrogen bases yields 'normal' Brønsted coefficients, with $\beta \approx 0.5$.⁹ It is not just their relative acidities and proton transfer rates that make the nitroalkanes remarkable, they also exhibit rather large thermodynamic acidities, together with unexpectedly slow rates of proton transfer. For example, the rates for the water-catalysed ionization of nitroalkanes are six orders of magnitude slower than those for ketones of similar acidity and ten orders of magnitude slower than those of normal acids.¹⁰

Nitroalkanes are a case study for proton transfers, and have provided the ground to test the applicability of old and emerging models in this area. The unusual effects observed in the catalysis of nitroalkanes have stimulated discussions, and alternative views exist in the literature. The current rationale is based on non-

equilibrium solvation along the RC, and/or the change in the intrinsic barrier to reaction within a series of nitroalkanes. It is important to mention the most relevant work in this area to give an adequate perspective.

Shortly after the publication of the first paper by Bordwell and co-workers on nitroalkanes, Marcus¹¹ offered an explanation for the anomaly in terms of his theory for proton transfers. According to this, the free energy barrier of a reaction, ΔG^\ddagger , can be expressed in terms of an intrinsic barrier, ΔG_0^\ddagger [$= \Delta G^\ddagger (\Delta G^0 = 0)$], and the free energy change of the reaction ΔG^0 :

$$\Delta G^\ddagger = \Delta G_0^\ddagger [1 + \Delta G^0 / (4\Delta G_0^\ddagger)]^2 \quad (2)$$

Assuming that the intrinsic energy barrier remains constant along the reaction series, the Brønsted coefficient, $d\Delta G^\ddagger / d\Delta G^0$, is given by

$$\alpha = \frac{1}{2} [1 + \Delta G^0 / (4\Delta G_0^\ddagger)] \quad (3)$$

This approach is equivalent to calculating ΔG^\ddagger for the proton transfer reaction $\text{AH} + \text{B}$ as the average of the intrinsic barriers for the exchange reactions $\text{AH} + \text{A}$ and $\text{BH} + \text{B}$ (the arithmetic mean assumption). If the intrinsic barrier for a series of substituted acids or bases changes appreciably, an extra term must be included, and α can be outside the normal range. This happens when the substituent induces significant structural reorganization, either intramolecular or due to solvation, and the intrinsic barrier for the corresponding exchange reaction is high. The variation of ΔG_0^\ddagger along a reaction series corresponds to the inclusion of a second progress variable, in addition to ΔG^0 , the sole variable considered in the original application by Marcus. Rose and Stuehr¹² utilized Marcus theory to estimate the changes in the intrinsic properties of internally hydrogen-bonded weak acids in their deprotonation by hydroxide ion. Unfortunately, as the authors recognized, all the parameters involved (ΔG_0^\ddagger , ΔG^\ddagger , $d\Delta G_0^\ddagger / d\Delta G^0$) are taken from the experimental data, hence the calculated changes are made equal to the experimental values.

Kresge⁶ provided an explanation for the observed α values considering that field and hyperconjugation interactions have opposing effects on the energies for the equilibria, and for transition states. His analysis was based only on interactions between a nitroalkane and a base, and neglected solvent effects.

Bordwell *et al.*⁵ also presented an explanation for the anomalous coefficients measured at their laboratory. They postulated that the deprotonation occurs via the slow formation of a hydrogen-bonded pyramidal nitrocarbanion, which is subsequently converted into a planar nitronate ion. This suggestion was later shown to be inconsistent with carbon isotope effects,¹³ which revealed that rehybridization must be significant at the transition state. Further, Bordwell *et al.* made the prediction that ketones in protic solvents should also give

anomalous Brønsted coefficients, which was not supported by later experiments with ketones.¹⁴

Pross and Shaik¹⁵ used their configuration mixing model to show that, even in a one-step process, the character of the transition state is not necessarily intermediate between that of reactants and products. Differences occur when a third configuration, distinct from those dominant in the reactants and products, makes a large contribution to the transition state (TS). Yamataka and Nagase¹⁶ carried out *ab initio* MO calculations for hydrogen atom transfers from R—H to X· and showed that the TS varies in the Leffler–Hammond manner when X = H, but does not vary appreciably when X = Cl. Endothermicity is evidently not the sole factor controlling the extent of TS variation. As the intrinsic barriers when X = Cl are smaller than those when X = H, these calculations contradict the predictions based on Marcus theory, which point towards smaller TS structure variations for reactions with a large intrinsic barrier. Alternatively, different degrees of charge separation when X = Cl or H were suggested as the source of the different behaviours of the calculated TS. It was considered that this charge separation, which is not present in either reactants or products, could be the source of the anomalous Brønsted coefficients.

Grunwald¹⁷ extended the unidimensional Marcus theory to incorporate a second progress variable, which for deprotonation of nitroalkanes was defined as the electronic rearrangement, assumed to be orthogonal with proton transfer. The use of a second coordinate is convenient to explain the disparity of two reaction events at the transition state, presumed to be the source of coefficients which do not conform to Hammond postulate. However, a simple calculation of such perpendicular effects¹⁸ showed that, in the calculated transition state, electronic rearrangement precedes proton transfer. This is contrary to experimental evidence. One way to reverse this is to add solvent reorganization to the disparity coordinate. The inclusion of the solvent in the RC is supported by the less anomalous coefficient observed for a series of arylnitromethanes in dimethyl sulphoxide (Me₂SO) ($\alpha = 0.92$),¹⁹ a poorer anion-solvating medium than water ($\alpha = 1.5$).⁹ The coefficient obtained in Me₂SO must be interpreted with care because it presumes that there is a negative deviation from the Brønsted correlation for the *p*-CN- and *p*-NO₂-substituted arylnitromethanes, whereas there is none for the *m,m'*-dinitro compound. A relatively weak resonance interaction of the *para* substituents in the 'pyramidal' transition state as opposed to the specially strong through-resonance in the planar nitronate anion was invoked to explain the deviations. This reasoning is not consistent with the carbon isotope effects mentioned above. Alternatively, the *m,m'*-dinitro compound can be seen as shown a positive deviation,²⁰ and the other

substituents define a curved Brønsted plot in Me₂SO. Based on the solvent effects and the normal behaviour of dinitroalkanes, Agmon²⁰ proposed that the anomalous coefficients observed in aqueous solutions are due to the variation of the work terms, caused by variations in the hydrogen bond strengths within the reaction series, with the free energy of proton transfer. Actually, the pK_a increase of phenylnitromethane when the solvent is changed from water to water–Me₂SO (10:90) is due to the destabilization of the carbanion (22.9 kJ mol⁻¹), and the stabilization of the carbon acid (-16.0 kJ mol⁻¹), only partially compensated by the destabilization of H⁺ (-17.1 kJ mol⁻¹).²¹ When the water content of the solvent is decreased, the effect of the loss of hydrogen bonding in the aromatic organic anion is comparable to the stronger solvation of the aromatic organic acid in their contribution to the lowered thermodynamic acidities.

One of the most complete studies of solvent effects on Brønsted coefficients and intrinsic rate constants for nitroalkanes deprotonation was made by Bernasconi.²² He formulated the principle of non-perfect synchronization,²² according to which a product stabilizing factor (resonance or solvation) lowers the intrinsic reaction rate if it develops late, relative to the transfer of the negative charge from the base to the carbon acid, but enhances the rate if it develops early. The late development of solvation relative to the development of the nitronate ion at the transition state was believed to be the main cause of the increase in the intrinsic rate constants with the increase in the Me₂SO content of the solvent. Essentially the same reason was invoked to explain the variation of the disparity of Brønsted coefficients ('imbalances') in nitroalkanes with the solvent. Such imbalances are understood as the difference between the variation of the deprotonation rates with the pK_a of the carbon acid (measured by α_{CH}) and with the pK_a of the base (measured by β_B), $\alpha_{CH} - \beta_B$, assuming that β is a rough measure of bond formation or charge transfer at the transition state.²³ The effect of resonance was assessed by comparing nucleophilic additions to the sp² carbon of β -nitrostyrenes with proton transfer to the sp³ carbon of ring-substituted 1-phenyl-2-nitroethanols. The smaller imbalances observed in nucleophilic reactions were, in part, assigned to the fact the sp² carbon may keep its hybridization in the course of the reaction, facilitating the shift of charge into the nitro group and keeping the reaction synchronous. For proton transfers, an additional imbalance enhancing factor may be hydrogen bonding between the base and the proton which is in flight, facilitated by the localization of charge in the carbon atom.⁷ This mechanism, favouring the localization of charge in the carbon, is similar to that proposed by Bordwell *et al.* However, the argument on rehybridization is not supported by carbon isotope effect studies.¹¹

Kurz²⁴ considered that the solvent effects on the intrinsic rate constants could result both from a change in the equilibrium constant for the formation of the AH, B^- precursor complex, as suggested by Agmon,²⁰ and a change in the rate constant for proton transfer, as formulated by Bernasconi and co-workers.²¹⁻²³ The first effect results from the desolvation of B^- accompanying the formation of the precursor complex, and is designated as a work term in the theory of Marcus. The second effect results from the effective relaxation time for orientational solvent polarization in the neighbourhood of a reaction event (one of the components of solvation), being two orders of magnitude less than the lifetime of the vibrational motion corresponding to the acid-base proton transfer. This difference in response times may lead to an asynchrony between transfer of charge and reorganization of the solvation, which could result in non-equilibrium solvation of the transition state. Kurz's model, based on charge-containing ellipsoidal and spherical cavities in dielectric continua, showed that the two effects may have comparable magnitudes in water-Me₂SO mixtures.

Bunting and Stefanidis²⁵ modified the Marcus theory to include an empirical dependence of the intrinsic barrier on the free energy for reaction:

$$\Delta G_0^* = A + B \Delta G^0 \quad (4)$$

This empirical relationship was applied to a large number of reactions. Later, these authors²⁵ associated B with the work terms of the Marcus theory and called the A parameters the 'true' intrinsic barriers. This is analogous to Agmon's suggestion²⁰ that work terms may change with ΔG^0 . It is interesting that, in a series of reactions, replacing equation (4) in equation (2) makes ΔG^* remain a function of a single variable, ΔG^0 , but increases the number of adjustable parameters to two.

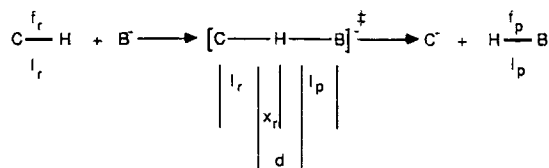
The above studies seem to indicate that interactions are present in the transition state that cannot be adequately modelled by their effect on equilibria. This poses severe restrictions on the applicability of physical organic models, designed to rationalize structure-reactivity relationships, which use data on stable structures (the only type of reliable information currently readily available for these systems) to predict transition-state structures and energies. Thus, an adequate description of nitroalkane deprotonations needs to incorporate a quantitative relationship between a parameter representing a variable transition-state property and a reactivity index obtainable from equilibria measurements, in addition to the dependence of the rates on the reaction free energies. The intersecting state model, described next, relates reaction rates to variable transition-state bonds orders and to ΔG^0 .

THEORY

The intersecting-state model (ISM) has been discussed

in detail elsewhere.^{27,28} Only its key features relevant to proton transfer reactions will be addressed here. This model considers that the activation energy of a reaction can be adequately calculated from the energetic variation occurring in the bonds of reactants and products that suffer major geometry and/or frequency changes in the course of the reaction. In carbon acid deprotonation by oxygen or nitrogen bases, these bonds are, in general, the C—H bond in the reactants and an O—H or N—H bond in the products. Within ISM, each reactive bond can be approximated by a diatomic harmonic oscillator, and its internal energy variation determined by its stretching force constant. The calculation of the activation energy for a reaction requires the knowledge of the displacement of reactants and products along the reaction coordinate, in addition to the reactive bond force constants, and the energy difference between reactants and products. Force constants are frequently available from spectroscopic data. Reaction energies can be calculated from tabulated carbon acid and oxygen/nitrogen base acidity constants. The displacement between reactant and product equilibrium geometries can only be obtained from a model-dependent progress variable. ISM defines the RC as the geometric distortion of reactive bonds of reactants and products from their equilibrium geometries to a position corresponding to the transition-state energy. Scheme 1 offers a unidimensional, and collinear, representation of the geometric changes involved in the RC. The model attempts to reproduce the variation in the energy of the transition states along the reaction series, and not the corresponding geometries.

The reaction path, d , can be obtained from two fundamental assumptions, one relating the transition-state bond order to electronic changes and the other associating the position of the TS with the free energy for the reaction. According to the first assumption, there is a strong correlation between changes in the bond being broken and the bond being formed in the course of reaction. This is also the basic assumption of the BEBO model,²⁹ and is equivalent to considering that the bond order is conserved along the reaction path, $n_{CH} + n_{BH} = 1$. This electronic condition for the energy variation along the reaction coordinate leads to an average transition-state bond order of $n^* = 0.5$. Later it will be shown that this condition can be relaxed, and variable n^* values can be obtained. A more general meaning is then attached to n^* .



Scheme 1

Usually, in a potential energy surface, the reactants and products valleys are tighter than the transition-state region, and the reaction coordinate d underestimates the total distortion of the reactive bonds at the transition state, $\Delta l_{TS} = \Delta l_r + \Delta l_p$ (Figure 1). For the $H + H_2$ reaction [Figure 1(a)],^{30a} the bond distension at the transition state is underestimated by 10–15%, which is acceptable given the major approximations involved. The condition $d \leq \Delta l_{TS}$ comes from the use of energetic, and not geometric, criteria to calculate reaction rates. The total distortion from equilibrium to TS geometries increases with the asymmetry of the potential energy surface (PES), of which the $F + H_2$ is an example [Figure 1(b)].^{30b} If no other conditions were applied, ISM should give increasingly worse results as $|\Delta G^0|$ increases. A second assumption is required to calculate activation energies for reactions involving large changes in ΔG^0 . ISM postulates that the effect of $|\Delta G^0|$ on d must be weighted by a parameter $1/\lambda$, such that λ is expressed in energy units and is positive. This thermodynamic condition for the variation of d allows for an extra increase in the bond distensions with the increase in $|\Delta G^0|$. For similar PES, i.e. for series of reactions, λ must be constant. For PES with tighter (lower entropy) transition states, a large variation in energy can be attained with a small displacement from the equilibrium positions, and d must be subject to a larger correction (lower λ) than for PES with looser (higher entropy) transition states. Thus, λ is expected to vary from one series of reactions to another, and to be related to the transition-state entropy. However, the model does not offer, at present, a method for the *a priori* calculation of λ . This parameter must be treated as an adjustable parameter, which characterizes each series of reactions. Koepl and Kresge³¹ approached this issue from a different perspective, but also suggested a quadratic dependence of d on ΔG^0 .

This work is focused on the calculation of proton transfer rates within series of substituted carbon acids. The absolute and relative free energy variations along each series are relatively small compared with the typical λ values for proton transfers from carbon acids. Within each nitroalkane series the ΔG^0 range is smaller than 30 kJ mol^{-1} ($7.2 \text{ kcal mol}^{-1}$), and when the proportion of water in the solvent is larger than 50%, it is typical to find $\lambda > 200 \text{ kJ mol}^{-1}$.³² Thus, to a first approximation, we can assume that $\lambda \gg |\Delta G^0|$, and that substituents can only exert a weak influence in the RC through a factor involving $\Delta G^0/\lambda$.

Mathematically, ISM gives the reaction coordinate as proportional to the sum of the equilibrium bond lengths of reactant and product:

$$d = \eta(l_r + l_p) \quad (5)$$

The reduced bond extension, η , is modulated by the transition-state bond order, n^* , and the 'mixing

entropy' parameter, λ , in addition to a (presumed) universal constant, $a' = 0.156$, and the free energy of the reaction:

$$\eta = (a' \ln 2/n^*) + (a'/2)(\Delta G^0/\lambda)^2 \quad (6)$$

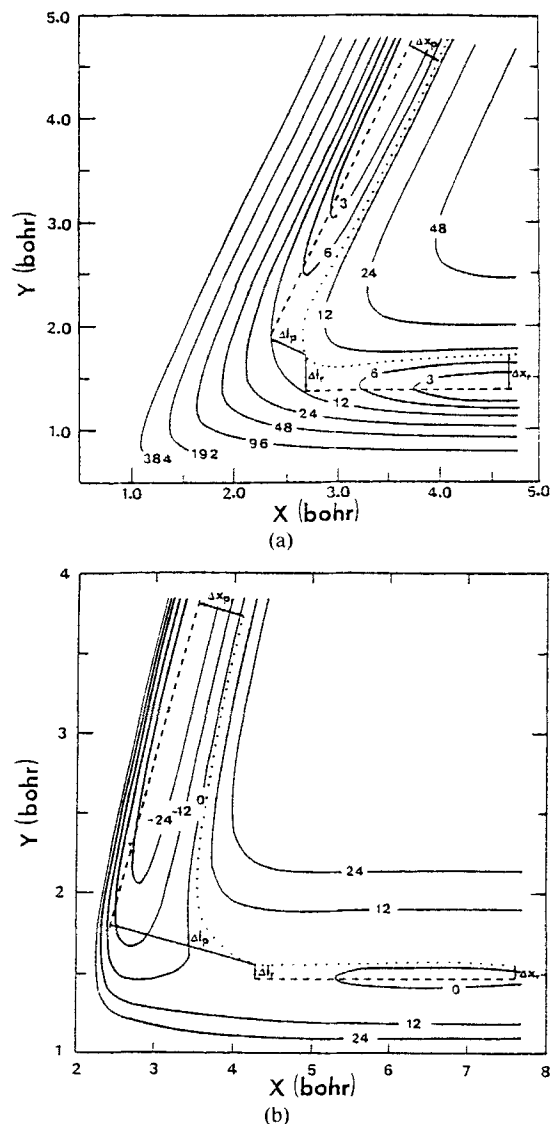


Figure 1. The solid curves represent the potential energy surfaces for the collinear reactions: (a) $H + H_2$, from Ref. 30a, and (b) $F + H_2$, from Ref. 30b. Their contours are marked in kcal mol^{-1} . The X-axis refers to the distance between the atom and the centre of mass of H_2 and the Y-axis to the distance between the two hydrogen atoms of H_2 . The geometric displacements, dictated by the PES, from the equilibrium positions to the transition-state geometry are qualitatively shown by Δl_r and Δl_p , and the equivalent displacements modelled by ISM are illustrated by Δx_r and Δx_p .

The energy profile can now be calculated, and the intersection of reactants and products potential energy curves is given by (Figure 2)

$$\frac{1}{2}f_r x_r^2 = \frac{1}{2}f_p (d - x_r)^2 + \Delta G^0 \quad (7)$$

This intersection gives the free energy of activation, $\Delta G^\ddagger = \frac{1}{2}f_r x_r^2$, which is needed for inclusion in the Eyring equation:

$$k = (k_B T/h) C_0^{1-m} \exp(-\Delta G^\ddagger/RT) \quad (8)$$

where $C_0 = 1 \text{ M}$ is the standard concentration and $m = 2$ the molecularity of the reaction, to calculate the proton transfer rate.

In 1987, Formosinho applied ISM to general proton transfer reactions³³ and to the deprotonation of HCN.³⁴ Next, the model was used to rationalize excited-state proton transfers.³⁵ Yates³⁶ endorsed the application of ISM to acid–base catalysis of organic photoreactions, a field where the Marcus theory does not give realistic results. The model was also applied to the acid–base catalysis of proton transfers from carbon acids.³² This later application was centred on rates of catalysis of a carbon acid by a series of oxygen/nitrogen bases and did not address the issues raised by the nitroalkanes. In a sense this work is an extension and generalization of the previous one, showing how the same concepts can be generalized to all proton-transfer reactions.

The first aspect to emphasize with nitroalkanes is that the reaction coordinate cannot be uniquely defined by the C–H and H–X (X = O, N) bonds. In the product configuration the negative charge is preferentially located in the oxygen atoms, rather than in the acidic carbon. This implies the participation of the nitro group in the reaction coordinate. In order to keep the

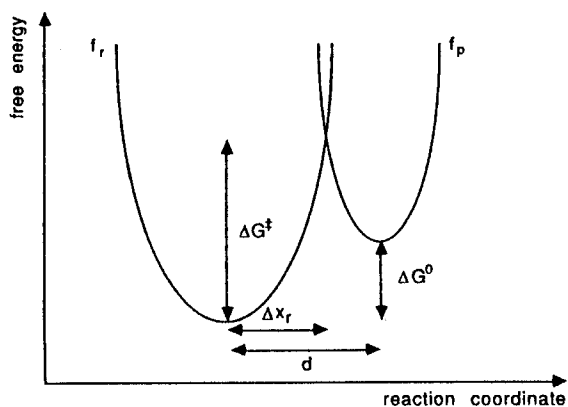


Figure 2. Representation of the reaction coordinate according to the intersecting-state model. The force constants for reactants and products are f_r and f_p ; Δx_r is the reactants bond distension and d is the total bond distension to the TS; the free energies for reaction and activation are ΔG^0 and ΔG^\ddagger

model unidimensional, it is necessary to represent the two NO and the CN oscillators of the nitro group together with the CH oscillator for the reactants, and proceed in a similar fashion for the products. As suggested for similar systems, the contribution of the nitro group is seen as an average of the CN and two NO force constants, distributed among the three bonds,³⁷ and the reactant force constant is estimated assuming that the CH and nitro oscillators behave as independent local modes.^{28,34}

$$f_{\text{NO}_2} = (f_{\text{CN}} + 2f_{\text{NO}})/3 \quad (9a)$$

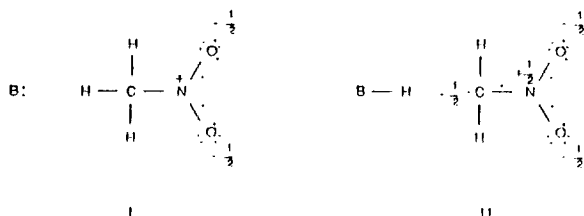
$$f_r = (f_{\text{CH}^2} + f_{\text{NO}_2})^{1/2} \quad (9b)$$

Using spectroscopic data for nitromethane,³⁸ one obtains $f_{\text{NO}_2} = 480 \text{ J mol}^{-1} \text{ pm}^{-2}$, which, together with $f_{\text{CH}} = 310 \text{ J mol}^{-1} \text{ pm}^{-2}$,³⁹ yields $f_r = 570 \text{ J mol}^{-1} \text{ pm}^{-2}$. In order to estimate the force constants for the products, we assume that the nitronate group can be represented by the same force constant as the nitro group, and use $f_{\text{OH}} = 420 \text{ J mol}^{-1} \text{ pm}^{-2}$ (or $f_{\text{NH}} = 380 \text{ J mol}^{-1} \text{ pm}^{-2}$),³⁹ to obtain $f_p = 640 \text{ J mol}^{-1} \text{ pm}^{-2}$ (or $f_p = 610 \text{ J mol}^{-1} \text{ pm}^{-2}$). The bond lengths, required by equation (5), can be estimated in a similar fashion. The average of the three nitro group bonds gives $l_{\text{NO}_2} = 129 \text{ pm}$,³⁸ and the average of this value with $l_{\text{CH}} = 109 \text{ pm}$ gives $l_r = 119 \text{ pm}$.³⁹ Identically, for products we obtain $l_p = 113 \text{ pm}$ with $l_{\text{OH}} = 96 \text{ pm}$ and $l_p = 115 \text{ pm}$ with $l_{\text{NH}} = 101 \text{ pm}$. This is an admittedly crude approximation to the weight of the nitro group in the reaction coordinate, but the variation in the force constants is partially compensated by the variation in the bond lengths and, as will be shown later, the relative rates of proton transfers calculated are not very sensitive to the force constant and bond length values.

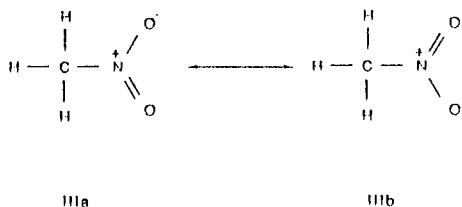
However, absolute rates can be very sensitive to the magnitude of the force constants involved. In a concerted reaction path such as that presumed above, the proton transfer to the base and the delocalization of the negative charge to the nitro group take place in a single kinetic step. Dewar⁴⁰ has shown that, in general, a synchronous multi-bond mechanism leads to a larger activation energy than an equivalent mechanism where the bond reorganization occurs in discrete steps. Within ISM, this is reflected by the increased force constants. The synchronous reaction path can only become competitive if its electronic rearrangement compensates the nuclear rearrangement. According to Woodward–Hoffmann rules, this can be achieved through transition structures with ‘aromatic’ resonance.⁴¹ In terms of ISM, this is seen as the result of an enhanced n^\ddagger value.³⁷ There is a subtle difference between concerted and synchronous reaction paths. In the former, nuclear and electronic rearrangements may not take place in unison, although no intermediate is involved. This seems to be the case in nitroalkane deprotonation, where the electronic rearrangement lags behind the

proton transfer but the acidic carbon rehybridization is extensive at the transition state.

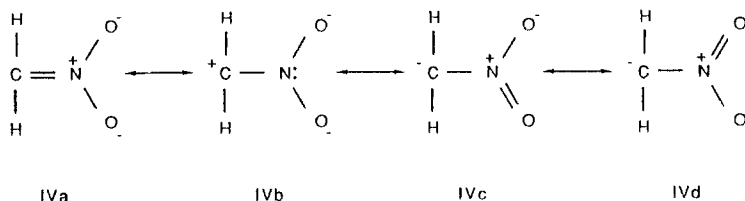
For a symmetric, and synchronous, bond-breaking and bond-forming process, n^\ddagger must be close to 0.5. Values ranging from 0.51 to 0.64 were obtained in the previous application of ISM to carbon acid catalysis. When the nitro group is included in the reactive bonds, their valence is increased by an extra electron. This can be visualized by the increased valence structures, **I**, for the reactants, and **II**, for the products. Structure **I**



emphasizes the equality between the two NO bonds in the reactants, given by the conventional Lewis structures **IIIa** and **IIIb**. Structure **II** makes the distribution



of the extra electron in the anion particularly clear. This is also illustrated by the valence structures **IV**, which distribute the charge unevenly between four atoms. Among these, **IVa** is the most important configuration.²¹ The carbon-centred anion is represented by structures **IVc** and **IVd**, which have the effect of reducing the negative charge on the oxygen atoms.⁴³ The structure **IVb** is believed to be an important con-



figuration when polar and hyperconjugative interactions operate (substitution of H by CH_3).^{5,6}

As the bonding effect of the extra electron must be shared by the two oscillators considered in our analysis (i.e. the CH or OH and the nitro oscillators), n^\ddagger must

increase by 0.25. Hence, for proton transfers involving the nitro group, one may expect $n^\ddagger = 0.75$. A transition-state bond order increase due to the participation of substituent groups in the reaction coordinate was also observed in HCN.³⁴

An increase in the bond order at the TS is in apparent contradiction with the BEBO model and some of its extensions,⁴⁴ which were successful in postulating the conservation of the bond order along the reaction path. This approximation has been supported by dynamic and *ab initio* calculations.^{45,46} Actually, Lendvay⁴⁶ has shown that the bond order of the making bond at the TS and the Brønsted coefficient α have a parallel variation with the reaction free energy. This raises the interesting issue of how that analogy could hold in the case of anomalous α values. In their pioneering work with the BEBO model, Johnston and Parr²⁹ already identified problems with the application of the model to halogen atom reactions. Also, in some unsymmetrical atom-transfer reactions the inflection point in the bond order profile does not coincide with the saddle point in the corresponding energy plot.⁴⁷ Recent *ab initio* studies showed that electronegativity differences between the end atoms in Scheme 1 lead to polar transition states,¹⁶ and the resulting charge separation was claimed to be the source of enhanced α values. Shi and Boyd⁴⁸ reinforced this interpretation and added that the electronic structure of the TS is another factor influencing its charge development. This second factor results from the significant contribution of higher energy configurations to the TS, and is in agreement with Pross and Shaik's valence bond configuration mixing model.¹⁵ The increased valence structures presented above attempt to mimic the effect of the configuration mixing, and are the basis for calculating n^\ddagger , the parameter that characterizes the transition-state electronic structures within ISM.

There is one more peculiarity of nitroalkanes. As seen in Figure 3, for the series CH_3X , with X = H, Cl, CN, COCH_3 , C_6H_5 and NO_2 , nitromethane has a remarkably high electron affinity and, in this series, only its anion is stable in the gas phase. The LUMO

energies of more substituted nitroalkanes, such as $\text{C}_6\text{H}_5\text{CH}_2\text{NO}_2$ or $\text{CH}_2(\text{NO}_2)_2$, will exhibit an even greater stabilization relative to nitromethane. As the LUMO (SOMO in the products) energy is reduced, its contribution to the transition-state configuration will

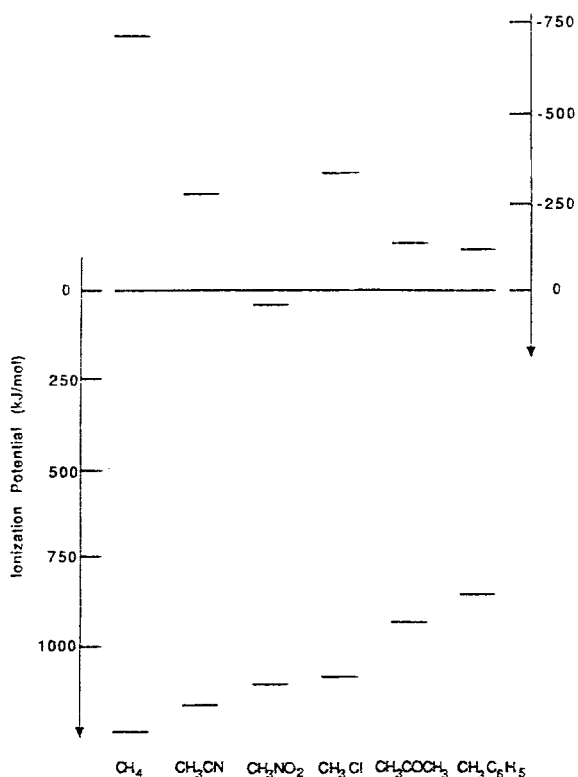


Figure 3. HOMO energies, as given by the vertical ionization potentials from Ref. 62, and LUMO energies, obtained from the electron affinities in Ref. 63

increase. This effect shows up particularly in nitroalkanes because of the energetic stabilization of the carbanion. Thus, the extent of its extra electron contribution to an increase in n^\ddagger depends on the stabilization induced by the substituent. This reasoning predicts a positive correlation between electron affinities and transition-state bond orders, which is consistent with our previous work in this area.³²

Unfortunately, electron affinities are not, in general, available for carbon acids. This can be circumvented by making use of parameters measuring substituent effects on electron affinities. For example, there is a good correlation between relative electron affinities and gas-phase acidities.⁴⁹ Further, it is useful to recall that σ parameters reflecting independent resonance, field/inductive and polarizability effects can account for relative gas-phase proton-transfer acidities.⁵⁰ Hence, a correlation between electron affinities and such σ parameters should be obtained. In fact, a correlation between electron affinities and σ_p^- Hammett substituent constants has been suggested.⁵¹ A similar correlation was found between oxidation potentials, related to

ionization potentials, and Hammett σ^+ parameters.⁵² The success of the correlations with σ parameters can be attributed, in part, to the proportionality between the sensitivity of the reactions to resonance effects and the *ab initio* π charge density on the acidic carbon of the unsubstituted parent acid structure.^{50,53} All this evidence in favour of a correlation between the electronic density at the acid carbon atom and constants dependent only on the substituent, derived from Hammett σ parameters, gives us confidence to propose a correlation between n^\ddagger and σ parameters; but which σ parameters?

In 1968, Swain and Lupton⁵⁴ collected more than 20 different sets of σ constants. In this work, it was possible to show that, in solution, each σ set is a linear combination of only two basic σ sets, F and R , which measure field/inductive and resonance capabilities of the substituents. This work was updated in 1983,⁵⁵ and we use Swain *et al.* F and R substituent constants to correlate our n^\ddagger values. Taft and co-workers^{50,53} followed a similar approach, interpreting relative gas-phase acidities in terms of appropriate combinations of dipolar field/inductive (F), π electron delocalization (R) and polarizability (P) effects. Considering that polarizability effects are completely attenuated in aqueous solutions,^{56,57} it is evident that the approaches of Swain's and Taft's groups are equivalent.

ISM and BEBO models assign different meanings to the transition-state bond order. For BEBO, n^\ddagger translates electronic correlation between the bonds being broken and formed and, through the Pauling relation,⁵⁸ the model gives the nuclear geometries at the critical configuration. Within ISM, additional electronic factors are considered in the determination of n^\ddagger , such as ionic configurations, polar effects and π electron delocalization, and this model is more adequate to calculate the transition-state energies.

For nearly thermoneutral nitroalkane deprotonations, it is possible to calculate absolute activation energies taking $n^\ddagger = 0.75$, $f_r = 570 \text{ J mol}^{-1} \text{ pm}^{-2}$, $f_p = 640 \text{ J mol}^{-1} \text{ pm}^{-2}$ (or $f_p = 610 \text{ J mol}^{-1} \text{ pm}^{-2}$), $l = 232 \text{ pm}$ (or $l = 234 \text{ pm}$) and the carbon acid and base catalyst experimental $\text{p}K_a$ values. Such a calculation does not make use of any adjustable parameters, and is useful to assess the validity of the approximations made. In the study of relative kinetic acidities, it is better to adjust n^\ddagger in order to reproduce the experimental deprotonation rates, and correlate their variations with resonance (R) and field/inductive parameters (F). When used to rationalize experimental observations, the model acquires an essentially interpretative value. The model can also be used to establish trends in the data, hence, despite its empirical nature, having a predictive value.

Before ISM is applied, it is important to clarify the criteria used to account for statistical factors. The deprotonation rate per equivalent acidic hydrogen and

per equivalent basic point is

$$k_d = k_{d,exp}/(p_A q_B) \quad (10)$$

where p_A and q_B are the number of acidic hydrogens and basic sites, respectively. For the reverse reaction, a similar correction must be made, giving $k_p = k_{p,exp}/(p_B q_A)$. These determine the correction to be

made to the reaction free energy:

$$\Delta G^0 = -2 \cdot 303RT \{ pK_a^{BH} + [\ln(p_B/q_B)]/2 \cdot 303 - pK_a^{CH} - [\ln(p_A/q_A)]/2 \cdot 303 \} \quad (11)$$

Correction for homoconjugation is also made, where appropriate.

Table 1. Deprotonation rates of nitroalkanes by lyate ion in methanol-water (50:50, v/v)^a

No.	GNO ₂ ^b	ΔG^0 (kJ mol ⁻¹)	k_d (l mol ⁻¹ s ⁻¹)	n^*
1	(CH ₂) ₃ SO ₂ C ₆ H ₅	-34.0	29	0.7807
2	(CH ₂) ₃ CN	-33.7	23	0.7779
3	(CH ₂) ₃ SC ₆ H ₅	-33.1	14	0.7729
4	(CH ₂) ₃ OC ₆ H ₅	-32.8	11	0.7707
5	(CH ₂) ₃ COCH ₃	-32.2	8.2	0.7691
6	(CH ₂) ₃ OH	-31.9	7.7	0.7691
7	(CH ₂) ₃ C ₆ H ₅	-31.2	5.5	0.7663
8	(CH ₂) ₃ CH ₃	-31.3	2.3	0.7567
9	(CH ₂) ₂ CH ₃	-30.4	2.4	0.7583
10	CH ₂ CH ₃	-32.3	2.8	0.7567
11	(CH ₂) ₂ C ₆ H ₅	-31.0	8.2	0.7713
12	(CH ₂) ₂ OH	-28.1	40	0.7974
13	CH ₃	-24.2	15	0.7945
14	CH ₂ C ₆ H ₅	-41.7	72	0.7746
15	CH ₂ - <i>t</i> -C(CH ₃) ₃	-20.8	0.32	0.7562
16	CH(CH ₃)C ₆ H ₅	-41.2	3.5	0.7316
X-C ₆ H ₄ CH(CH ₃)NO ₂ ^b				
17	<i>p</i> -CH ₃	-41.0	2.4	0.7277
18	<i>p</i> -F	-42.1	5.8	0.7351
19	<i>p</i> -Cl	-42.9	8.6	0.7381
20	<i>p</i> -CF ₃	-43.9	18	0.7442
21	<i>p</i> -NO ₂	-47.1	72	0.7535
22	<i>m</i> -CH ₃	-40.6	2.5	0.7291
23	<i>m</i> -CH ₃ O	-41.4	4.4	0.7336
24	<i>m</i> -F	-42.9	10	0.7401
25	<i>m</i> -Cl	-43.0	12	0.7416
26	<i>m</i> -CF ₃	-43.5	17	0.7442
27	<i>m</i> -NO ₂	-45.7	43	0.7504
X-C ₆ H ₄ CH ₂ CH(CH ₃)NO ₂ ^c				
28	<i>p</i> -CH ₃ O	-37.3	0.78	0.7233
29	<i>p</i> -CH ₃	-37.3	0.80	0.7238
30	H	-37.7	0.94	0.7243
31	<i>p</i> -F	-38.1	1.2	0.7262
32	<i>p</i> -Cl	-38.2	1.4	0.7282
33	<i>p</i> -CF ₃	-38.8	2.1	0.7306
34	<i>p</i> -NO ₂	-39.8	3.6	0.7346
35	<i>m</i> -CH ₃	-37.4	0.84	0.7238
36	<i>m</i> -CH ₃ O	-38.0	1.0	0.7247
37	<i>m</i> -F	-38.3	1.7	0.7296
38	<i>m</i> -Cl	-38.5	1.7	0.7291
39	<i>m</i> -CF ₃	-38.4	2.0	0.7306
40	<i>m</i> -NO ₂	-39.3	3.2	0.7341

^a 1-15 from Ref. 5; 16-40 from Ref. 64.

^b At 288 K.

^c At 298 K.

RESULTS

Tables 1–5 show the results of the application of ISM to the deprotonation of several series of nitroalkanes by oxygen and nitrogen bases. The concentration of H₂O in pure water is taken as 55 M, giving $\text{p}K_a(\text{OH}^-) = 15.74$ and $\text{p}K_a(\text{H}_2\text{O}) = -1.74$. The n^* values presented were empirically adjusted to make the rates calculated by equations (4)–(7) agree with the statistically corrected, experimental deprotonation rate constants, k_d . Except where noted, it is assumed that $\lambda \gg |\Delta G^0|$. Within each series, the structural changes are relatively minor and n^* varies by less than 10%. Such small variations are responsible for factors of 10^3 in the rates. These tables cover a wide range of nitroalkane and

solvent systems, and are representative of the deprotonation reactions of this class of carbon acids.

Table 6 presents a more dramatic type of structural variation, where the substituents are directly bonded to the acidic carbon. Here, the range of rate constants covers six orders of magnitude, and the n^* values vary by 17%. However, ΔG^0 varies by less than 32 kJ mol^{-1} ($7.5 \text{ kcal mol}^{-1}$) and there is no apparent relationship between reaction energies and rates (Figure 4). It is important to note that by setting n^* to the theoretical value of 0.75, it is possible to calculate k_d without adjustable parameters. In Figure 5 we compare the experimental data in Tables 1–4 with the rates calculated with $n^* = 0.75$. We also calculate n^* for all these reactions using the simpler approximation that only CH

Table 2. Deprotonation rates of nitroalkanes by pyridine in methanol–water (50:50, v/v)^a

No.	GNO ₂	ΔG^0 (kJ mol ⁻¹)	$10^5 k_d$ (l mol ⁻¹ s ⁻¹)	n^*
41	(CH ₂) ₃ NO ₂	18.8	17	0.7452
42	(CH ₂) ₃ SO ₂ C ₆ H ₅	19.1	12	0.7421
43	(CH ₂) ₃ CN	19.4	11	0.7416
44	(CH ₂) ₃ SC ₆ H ₅	20.0	6.1	0.7366
45	(CH ₂) ₃ OC ₆ H ₅	20.3	4.8	0.7351
46	(CH ₂) ₃ OH	21.2	3.1	0.7326
47	(CH ₂) ₃ C ₆ H ₅	22.0	2.0	0.7301
48	(CH ₂) ₃ CH ₃	21.9	1.3	0.7252
49	(CH ₂) ₂ CH ₃	22.8	1.1	0.7252
50	CH ₂ CH ₃	20.8	1.4	0.7238
51	(CH ₂) ₂ C ₆ H ₅	22.2	3.0	0.7341
52	(CH ₂) ₂ OH	25.2	5.7	0.7478
53	CH ₃	29.2	4.0	0.7535
54	CH ₂ C ₆ H ₅	11.1	74	0.7437
55	CH ₂ - <i>t</i> -C(CH ₃) ₃	32.7	0.091	0.7214

^a From Ref. 5, at 298 K.

Table 3. Deprotonation rates of *meta*-substituted 1-arylnitroethanes (at 278 K) and arylnitromethanes (at 279 K) by OH⁻ in water^a

No.	<i>m</i> -X-C ₆ H ₄ CH(CH ₃)NO ₂	ΔG^0 (kJ mol ⁻¹)	k_d (l mol ⁻¹ s ⁻¹)	n^*
56	CH ₃	-48.9	5.4	0.7223
57	H	-49.4	6.5	0.7233
58	F	-51.4	14	0.7282
59	Cl	-51.4	18	0.7301
60	CF ₃	-51.9	18	0.7296
61	NO ₂	-53.5	43	0.7361
62	(NO ₂) ₂	-57.6	300	0.7509
<hr/> <i>m</i> -X-C ₆ H ₄ CH ₂ NO ₂ <hr/>				
63	CH ₃	-50.1	62	0.7462
64	H	-50.6	80	0.7478
65	Cl	-52.0	240	0.7578
66	NO ₂	-53.9	620	0.7658

^a From Ref. 9.

and OH (or NH) bonds intervene in the reaction coordinate. This leads to $f_r = 290 \text{ J mol}^{-1} \text{ pm}^{-2}$, $f_p = 420 \text{ J mol}^{-1} \text{ pm}^{-2}$ ($380 \text{ J mol}^{-1} \text{ pm}^{-2}$) and $l = 203.3 \text{ pm}$ (208.3 pm). The variations in n^\ddagger thus obtained parallel those observed with the participation of the nitro group in the RC. The absolute values of n^\ddagger approach 0.5, as expected, but we also obtain very low n^\ddagger values, e.g. $n^\ddagger = 0.466$, for reaction (87).

Tables 7 and 8 show some selected results obtained for ketones, for series of both small and large structural variations. The procedure utilized here is the same as that for nitroalkanes. As the negative charge in the carbanion is now expected to be more localized in the carbon acid, it is assumed that the CH and OH bonds are sufficient to determine the RC. The n^\ddagger values are close to 0.5, as expected. This approximation will

Table 4. Deprotonation rates of *meta*-substituted 1-arylnitroethanes and arylnitromethanes by morpholine in water at 278 K^a

No.	<i>m</i> -X-C ₆ H ₄ CH(CH ₃)NO ₂	ΔG^0 (kJ mol ⁻¹)	k_d (l mol ⁻¹ s ⁻¹)	n^\ddagger
67	CH ₃	-8.5	0.018	0.7361
68	H	-9.1	0.021	0.7366
69	Cl	-11.0	0.045	0.7406
70	NO ₂	-13.2	0.094	0.7442
71	(NO ₂) ₂	-17.3	0.47	0.7535
<hr/> <i>m</i> -X-C ₆ H ₄ C ₂ NO ₂ <hr/>				
72	CH ₃	-9.8	0.44	0.7691
73	H	-10.3	0.49	0.7691
74	Cl	-11.7	1.4	0.7785
75	NO ₂	-13.6	2.9	0.7836

^a From Ref. 9.

Table 5. Deprotonation rates of *meta*- and *para*-substituted arylnitromethanes by benzoate anion in dimethyl sulphoxide at 278 K^a

No.	X-C ₆ H ₄ CH(CH ₃)NO ₂	ΔG^0 (kJ mol ⁻¹)	k_d (l mol ⁻¹ s ⁻¹)	n^\ddagger
76	<i>p</i> -CH ₃	12.2	19	0.8907
77	H	10.5	33	0.8944
78	<i>p</i> -Br	5.2	260	0.9140
79	<i>m</i> -NO ₂	-0.9	2100	0.9322
80	<i>p</i> -CN	-5.1	3200	0.9242
81	<i>p</i> -NO ₂	-9.0	4000	0.9140
82	<i>m,m'</i> -(NO ₂) ₂	-9.4	55000	0.9689

^a From Ref. 19.

Table 6. Deprotonation rates of nitroalkanes by OH⁻ in water at 278 K^a

No.	R' R''CHNO ₂		ΔG^0 (kJ mol ⁻¹)	k_d (l mol ⁻¹ s ⁻¹)	n^\ddagger
	R'	R''			
83	H	COOC ₂ H ₅	-56.8	75 000	0.8242
84	H	H	-30.6	9.2	0.7626
73	H	C ₆ H ₅	-50.6	80	0.7478
85	H	CH ₃	-40.8	2.6	0.7291
86	CH ₃	NO ₂	-61.7	360 000	0.8369
66	CH ₃	C ₆ H ₅	-49.4	6.5	0.7233
87	CH ₃	CH ₃	-47.4	0.32	0.6981

^a 83 from Ref. 65; 84, 85 and 87 from Ref. 6; 86 from Ref. 66.

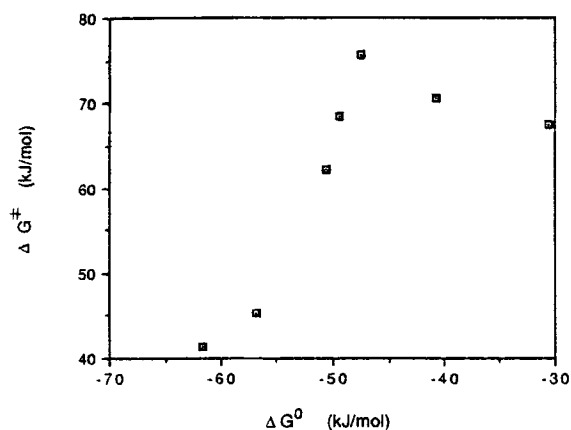


Figure 4. Brønsted type of plot with data from Table 6. The free energies of activation were obtained from the experimental rates, using $k_B T/h$ as a pre-exponential factor

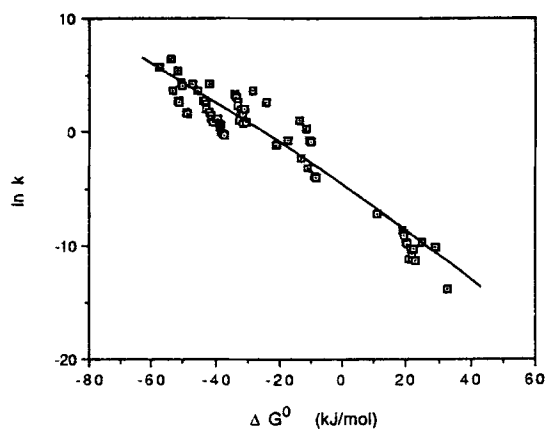


Figure 5. Brønsted type of plot with data from Tables 1–4. The theoretical curve was calculated according to ISM and making $n^* = 0.75$ and $\lambda \gg |\Delta G^0|$

underestimate the effect of the carbonyl group, but the relative n^* values within these series must be essentially correct.

Table 9 presents the results of the application of ISM to the proton transfer reactions between 9-alkylfluorene and (9-alkylfluorenyl)lithium in diethyl ether. In these calculations the phenyl group was taken as a single oscillator, just like the nitro group in the nitroalkanes, and its contribution to the RC was obtained by equation (9). The symmetry of the system leads to $f_i = f_p = 450 \text{ J mol}^{-1} \text{ pm}^{-2}$ and $l = 247 \text{ pm}$.

In Table 10 we present the calculated n^* values for the deprotonation of a large range of carbon acids by water. A quantitative treatment of these carbon acids as a reaction series is a novel situation in physical organic chemistry. The n^* values are seen to vary by more than 30%. Except for dinitromethane, the RC was considered to be defined only the CH and OH bonds.

Table 11 presents results for correlations of the form

$$n^* = n^*(0) + fF + rR \quad (12)$$

The physical meaning of $n^*(0)$ is, by definition, the value of the transition-state bond order when the substituent is the hydrogen atom; in the last correlation in Table 11, this corresponds to the deprotonation of methane by water. The values of F and R were taken from the work of Swain *et al.*;⁵⁵ f and r are adjustable parameters. The standard error of the estimate of each adjustable parameter is also presented.

It is important to emphasize that the reaction series $p\text{-XPhCH}_2\text{NO}_2$ in Table 11, whose n^* values are presented in Table 5, does not include the m,m' -(NO_2)₂ substituent. By the nature of F and R separation, *meta* and *para* substituents must have $n^*(0)$ in common, but may have different f and r parameters. In cases where two substituents are introduced in equivalent positions, their contributions to F and R were taken as additive.

When the carbon acid is kept constant and the oxygen/nitrogen base varies, the substituents are changed in remote places relative to the reaction centre

Table 7. Deprotonation rates of *para*-substituted 1-methyl-4-(*X*-phenylacetyl)pyridinium cation by OH^- in water at 278 K^a

No.	X	ΔG^0 (kJ mol ⁻¹)	k_d (l mol ⁻¹ s ⁻¹)	n^*
88	OCH ₃	-38.5	288	0.52620
89	H	-38.1	401	0.52980
90	CH ₃	-37.3	397	0.52807
91	Cl	-40.6	740	0.53158
92	CF ₃	-42.3	1340	0.53457
93	CN	-45.4	2620	0.53644
94	NO ₂	-47.7	3570	0.53612

^aFrom Ref. 14.

Table 8. Deprotonation rates of ketones by OH⁻ in water at 278 K^a

No.	R'CH ₂ COCH ₂ R''		ΔG^0 (kJ mol ⁻¹)	k_d (l mol ⁻¹ s ⁻¹)	n^+
	R'	R''			
95	H	COCH ₃	-39.3	20000	0.5667
96	H	COOC ₂ H ₅	-28.9	3400	0.5655
97	H	SO ₃ ⁻	-12.3	130	0.5606
98	H	H	21.3	0.042	0.5426
99	CH ₃	CH ₃	25.4	0.0095	0.5364

^aFrom Ref. 67; the kinetic data for 98 and 99 were taken from Ref. 68.

Table 9. Deprotonation rates of 9-alkylfluorenes by 9-alkylfluorenyl anions in diethyl ether at 298 K^a

No.	FIR' ⁻	FIR''	ΔG^0 (kJ mol ⁻¹)	10 ⁸ k_d (l mol ⁻¹ s ⁻¹)	n^+
100	H	H	0.0	1930	0.6337
101		Me	-1.7	715	0.6238
102		Et	1.7	270	0.6217
103		<i>i</i> -Pr	5.7	112	0.6202
104		<i>t</i> -Bu	9.5	25.9	0.6164
105	Me	Me	0.0	330	0.6202
106		Et	3.4	104	0.6167
107		<i>i</i> -Pr	7.4	32.1	0.6144
108		<i>t</i> -Bu	11.2	5.09	0.6061
109	Et	Et	0.0	51.1	0.6068
110		<i>i</i> -Pr	4.0	13.5	0.6035
111		<i>t</i> -Bu	7.8	0.820	0.5893
112	<i>i</i> -Pr	<i>i</i> -Pr	0.0	4.81	0.5912
113		<i>t</i> -Bu	3.8	0.501	0.5814
114	<i>t</i> -Bu	<i>t</i> -Bu	0.0	2.63	0.5679

^aFrom Ref. 8.

Table 10. Deprotonation rates of carbon acids in water at 298 K^a

No.	CH ₂ R ₂	ΔG^0 (kJ mol ⁻¹)	10 ⁵ k_d (l mol ⁻¹ s ⁻¹)	n^+
115	CH ₃ CH ₂ CO ₂	84.8	0.023	0.5670
116	CH ₃ CH ₂ SO ₂	78.5	15	0.6402
117	CN	71.7	26	0.6182
118	CH ₃ CO	59.7	15	0.5709 ^b
119	NO ₂	29.3	750	0.8981 ^c
				0.8229

^a115–118 from Ref. 10, pp. 118, 151; 119 from Ref. 69.

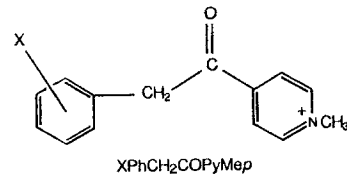
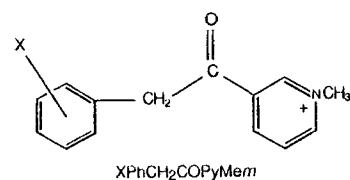
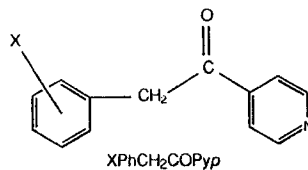
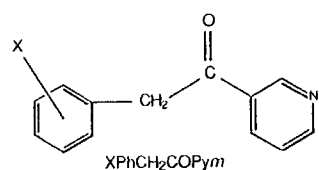
^bUsing $f_r = 290$ and $f_p = 420$.

^cUsing $f_r = 584$ and $f_p = 608$.

Table 11. Correlation of transition-state bond orders with field/inductive (F) and resonance (R) parameters^a

n_i	Series	$n^*(0)$	σ_n	$10^4 f$	$10^4 \sigma_f$	$10^4 r$	$10^4 \sigma_r$	r_c
9 ^b	G(CH ₂) ₃ NO ₂	0.7587	0.0143	216	23	8	8	0.9685
5 ^b	G(CH ₂) ₂ NO ₂	0.7552	0.0010	551	67	-87	20	0.9981
6 ^b	G'G''CHNO ₂	0.7950	0.0041	557	176	952	105	0.9831
6 ^b	<i>p</i> -XPhCHMeNO ₂	0.7312	0.0008	125	14	86	9	0.9954
7 ^b	<i>m</i> -XPhCHMeNO ₂	0.7313	0.0003	155	4	37	2	0.9991
8 ^b	<i>p</i> -XPhCH ₂ CHMeNO ₂	0.7246	0.0006	61	9	31	4	0.9876
7 ^b	<i>m</i> -XPhCH ₂ CHMeNO ₂	0.7244	0.0004	76	6	20	2	0.9944
9 ^c	G(CH ₂) ₃ NO ₂	0.7259	0.0008	171	12	13	4	0.9898
5 ^c	G(CH ₂) ₂ NO ₂	0.7239	0.0001	344	5	-43	2	1.0000
5 ^c	GCH ₂ NO ₂	0.752	0.038	702	149	664	113	0.9803
7 ^{d,e}	<i>m</i> -XPhCHMeNO ₂	0.7226	0.0009	109	14	28	10	0.9934
5 ^{f,e}	<i>m</i> -XPhCHMeNO ₂	0.7366	0.0005	64	9	18	7	0.9983
5 ^{g,e}	<i>m</i> -XPhCHMeNO ₂	0.7343	0.0002	73	4	18	2	0.9997
5 ^{h,e}	<i>m</i> -XPhCHMeNO ₂	0.7413	0.0012	80	23	22	19	0.9921
5 ^{i,e}	<i>m</i> -XPhCHMeNO ₂	0.7435	0.0003	66	7	12	6	0.9980
4 ^d	<i>m</i> -XPhCH ₂ NO ₂	0.7476	0.0002	147	5	31	4	1.0000
4 ^f	<i>m</i> -XPhCH ₂ NO ₂	0.7693	0.0003	132	6	10	5	0.9995
4 ^j	<i>m</i> -XPhCH ₂ NO ₂	0.76958	0.00003	126.4	0.6	7.9	0.5	1.0000
4 ^k	<i>p</i> -XPhCH ₂ NO ₂	0.8925	0.0052	297	109	-24	89	0.9446
7 ^l	R'R''CHNO ₂	0.7597	0.0034	408	81	665	49	0.9969
4 ^{d,m}	<i>p</i> -XPhCH ₂ COPym	0.5374	0.0002	36	3	21	2	0.9990
4 ^{d,e}	<i>m</i> -XPhCH ₂ COPym	0.5371	0.0008	54	13	12	10	0.9962
6 ^{d,n}	<i>p</i> -XPhCH ₂ COPyp	0.5331	0.0002	47	4	23	2	0.9970
7 ^d	<i>p</i> -XPhCH ₂ COPyMem	0.5378	0.0007	52	14	32	10	0.9847
7 ^d	<i>p</i> -XPhCH ₂ COPyMep	0.5297	0.0004	39	7	33	3	0.9923
5 ^{d,o}	R'CH ₂ COCH ₂ R''	0.5456	0.0020	5	93	255	49	0.9845
16 ^p	Fluorene/fluorenyl	0.6367	0.0054	2321	327	179	83	0.9475
4 ^q	R'R''CH ₂	0.098	0.197	190	1120	3310	1760	0.9472

^a F and R from Ref. 55; n_i is the number of elements in each series; $n^*(0)$ is the transition-state bond order when the substituent is the hydrogen; f and r are adjustable coefficients [equation (12)], and the corresponding standard errors of estimate are σ_n , σ_f and σ_r ; r_c is the correlation coefficient.



^b Reaction with lyate ion in water-methanol (50:50, v/v).

^c Reaction with pyridine in water-methanol (50:50, v/v).

^d Reaction with OH⁻ in water.

^e Including *m,m'*-(NO₂)₂.

^f Reaction with morpholine in water.

^g Reaction with diethylamine in water.

^h Reaction with piperidine in water.

ⁱ Reaction with piperazine in water.

^j Reaction with lutidine in water.

^k Reaction with benzoate ion in dimethyl sulphoxide.

^l Data from Table 6.

^m Excluding *p*-NO₂; with this substituent the correlation drops to 0.9307.

ⁿ Excluding *p*-NO₂; with this substituent the correlation drops to 0.9464.

^o Data from Table 8.

^p Data from Table 9, with n^* obtained as the average of the values adjusted to reproduce deprotonation and protonation rates, which agree within ± 0.001 ; *i*-Pr substituents were not used in the correlation because there are no F or R values tabulated for them.

^q Data from Table 10, excluding acetylacetone, for the reasons discussed in the text.

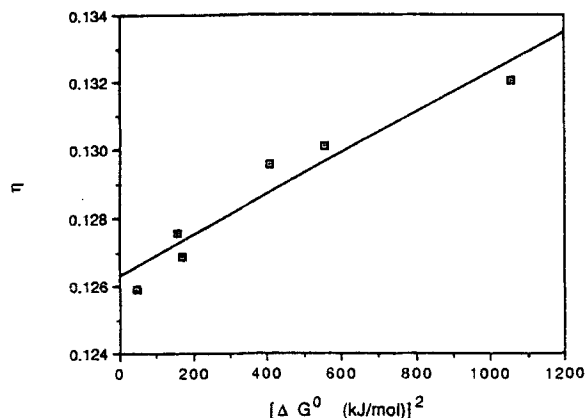


Figure 6. Reduced bond distortions, η , as a function of $(\Delta G^0)^2$, for proton transfers from phenylnitromethane to carboxylate anions in Me_2SO -water (90:10). Correlation coefficient: 0.963

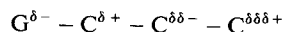
but large variations in ΔG^0 may occur. Under these conditions, the second term of equation (3) may become dominant, and a correlation between η and $(\Delta G)^2$ is expected. This is illustrated in Figure 6, using the data for the catalysis of phenylnitromethane by carboxylate anions in Me_2SO -water (90:10).²³ Other cases of such situations have been published.³²

DISCUSSION

In Tables 1-10, reactions are gathered which are usually not considered as belonging to the same Brønsted series. The sample of apparently unrelated rates and free energies in Figure 4 illustrates the data in Table 6. Table 11 contains the essence of our analysis. Its success can be evaluated from the usefulness of the establishment of a new type of relationship, distinct from the traditional rate-equilibrium relationships. According to this application of ISM, each reaction series is defined by common $n^*(0)$, f and r values and by the use of a common base and medium. The series are interrelated. For example, the series $\text{G}(\text{CH}_2)_2\text{NO}_2$ has compounds **8** and **9** in common with the series $\text{G}(\text{CH}_2)_3\text{NO}_2$ and also compounds **9** and **10** in common with $\text{G}'\text{G}''\text{CHNO}_2$; further, both this last series and XPhCHMeNO_2 include compound **16**. Identically, the series $\text{R}'\text{R}''\text{CHNO}_2$, which refers to deprotonations by OH^- in water, also overlaps in one case, **64**, with the series $\text{XPhCH}_2\text{NO}_2$, and in another, **57**, with XPhCHMeNO_2 . It is obvious that aromatic series which differ in the position of the ring substituent overlap in the unsubstituted parent compound and should have a common $n^*(0)$. Our results show that this is indeed the case.

It is also expected that, in saturated systems, the

resonance component of the substituent interaction should decay more rapidly with the distance from the acidic carbon than the field/inductive component. This can be seen comparing the values of f and r for series differing by one methylene linkage, such as $\text{G}(\text{CH}_2)_n\text{NO}_2$ and $\text{G}(\text{CH}_2)_{n-1}\text{NO}_2$, or $\text{XPhCH}_2\text{CHMeNO}_2$ and XPhCHMeNO_2 . Whereas f drops to ca half of its value when an extra CH_2 link is introduced, the decrease in r sometimes approaches one order of magnitude. It is interesting that r may acquire negative values which are statistically significant. This may be related to some theoretical calculations suggesting, in aliphatic compounds, a relay mechanism of the type⁵⁹



We note that $\text{G}'\text{G}''\text{CHNO}_2$ is not directly comparable with $\text{G}(\text{CH}_2)_n\text{NO}_2$, because it includes other effects in addition to the increase in the chain length. Excluding **16** from this series, f increases to 0.0618, with a standard error of the estimate of 0.0189. It is also interesting to see how ring substituents compare. Substitution in the *para* position always leads to weaker field/inductive and stronger resonance effects than in the *meta* position. The decrease in f is consistent with the increase in the distance from the acidic carbon. It is well known that substituents in the *para* position lead to particularly strong resonance interactions,¹⁹ which explain the enhanced r values.

As a corollary of the difference in the attenuation of F and R effects with distance, substituents directly attached to the acidic carbon may interact predominantly via their resonance effect. On the other hand, resonance must be negligible for substituents placed three carbon atoms away from the leaving proton. This is fully verified by our calculations. Figure 7 shows the

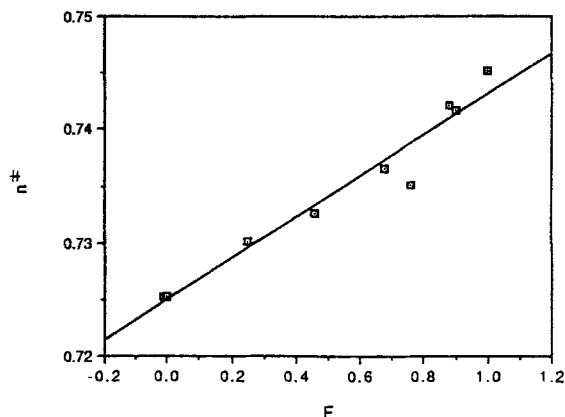


Figure 7. Transition-state bond orders, n^* , as a function of field/inductive parameters, F , in the deprotonation of $\text{G}(\text{CH}_2)_3\text{NO}_2$ by pyridine in methanol-water (50:50). Correlation coefficient: 0.975

quality of the linear correlation between n^* and F in the deprotonation of $G(\text{CH}_2)_3\text{NO}_2$ by pyridine. Figure 8 reveals the importance of resonance in the series $\text{R}'\text{R}''\text{CHNO}_2$.

The worse correlation presented in Table 11 refers to the deprotonation of $p\text{-XPhCH}_2\text{NO}_2$ by benzoate ion in dimethyl sulphoxide. It is not only its low correlation that is disturbing, but also the low value of r is unrealistic when compared with other *para*-substituted arylnitroalkanes. The correspondent Brønsted plot gives $\alpha = 0.65$, with a correlation coefficient of 0.985 (only the *para* substituents reported in Table 5 were considered), but is better described as a curvilinear relationship. It is clear that effects not properly accounted by F and R influence these deprotonation rates. It is tempting to assign the low correlation to through-resonance of the $p\text{-NO}_2$ and $p\text{-CN}$ substituents with the carbanion, and to expect a better correlation with σ^- parameters. However, resonance and field/inductive effects describe equally well σ^+ , σ and σ^- parameters.^{54,55} The claim that this kind of resonance can be more important in the planar products than in the pyramidal transition state is inconsistent with the TS rehybridization indicated by the carbon kinetic isotope effects.¹³

Another reason for the low correlation can be sought in the effect of $(\Delta G^0)^2$ on η , so far neglected. This may appear to be a weak argument because, for this series of reactions, the range of values involved, 150 (kJ mol^{-1})², is one of the lowest presented here. However, two factors contribute to make the $(\Delta G^0)^2$ effect on these reaction rates unique: the reactions take place in a non-aqueous solvent, and the sign of ΔG^0 changes within the series. It has been shown that λ may decrease by an order of magnitude when the content of Me_2SO

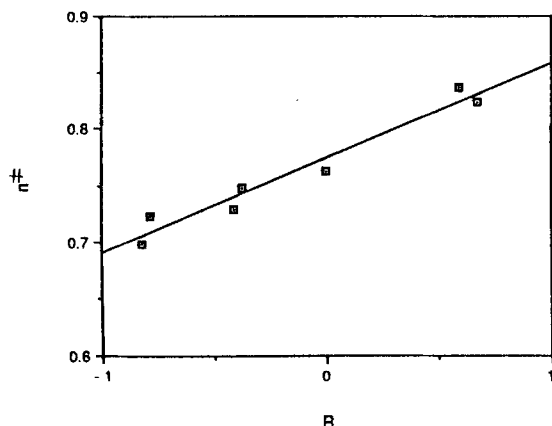


Figure 8. Transition-state bond orders, n^* , as a function of resonance parameters, R , in the deprotonation of $\text{R}'\text{R}''\text{CHNO}_2$ by OH^- in water. Correlation coefficient: 0.977

in an aqueous solution increases to 90%.³² Thus, the second term of the right-hand side of equation (6) may give a non-negligible contribution to η . Further, when the sign of ΔG^0 is maintained within a series, its effect on η is continuous and may reinforce or attenuate the effect of a variable n^* . In either case a small systematic error is introduced in the correlations of n^* with F and R , to which the correlation coefficients will not be very sensitive. In the present case, the η values of the $p\text{-Br-}$ and $p\text{-CN-}$ substituted arylnitromethanes will have a small contribution from the term in $(\Delta G^0/\lambda)^2$, while the other *para*-substituted compounds will have a much larger contribution from this effect. This will distort the correlation between n^* and F and R appreciably, because such variations in η are not linear with the trend induced by F and R effects.

In the deprotonation of carbon acids in solvent mixtures with high Me_2SO content, λ approaches 70 kJ mol^{-1} .³² This value can be used in the factor $0.078(\Delta G^0/\lambda)^2$ to obtain the values of n^* from the η values optimized to reproduce the deprotonation rates of phenylnitromethanes in Me_2SO . Using the n^* values calculated with this approximation to λ , we obtain

$$n^* = 0.908 + 0.015F + 0.003R$$

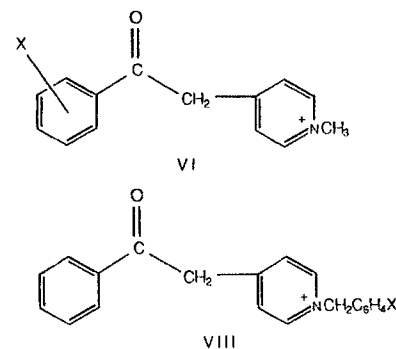
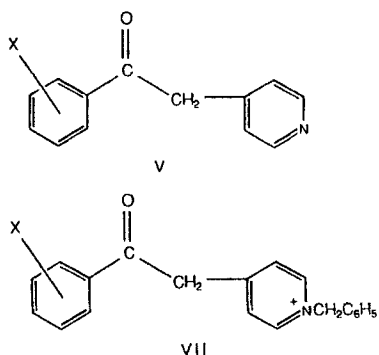
with a correlation coefficient of 0.967. This λ value seems to be appropriate, both because there is a precedent for it and because varying it by $\pm 5 \text{ kJ mol}^{-1}$ decreases the coefficient of the correlation of n^* with F and R . The appreciable improvement in the correlation with the inclusion of the ΔG^0 effect is indicative of its importance. Notwithstanding, the correlation is not completely satisfactory. Probably other factors may also play important roles. We note that the n^* values for $p\text{-CN}$ and $p\text{-NO}_2$ deviate negatively from the correlation defined by the other *para* substituents.

The series of aromatic ketones presented in Table 11 have remarkable similarities with the arylnitromethanes, namely the *para*-substituted compounds show stronger resonance effects whereas substituent field/inductive effects are more intense in the *meta* position. As expected from the lower electron affinity of acetone relative to nitromethane, the deprotonations of ketones admit smaller variations in n^* than those of nitroalkanes. Moreover, there is a conspicuous similarity between the effects of $p\text{-CN}$ and $p\text{-NO}_2$ in the deprotonation of arylnitromethanes and of aromatic ketones: the n^* values of $p\text{-CN-}$ and $p\text{-NO}_2\text{-}$ substituted aromatic ketones also deviate negatively from the correlation defined by the other compounds. This is also reflected in the Brønsted plots, where these compounds exhibit negative deviations.¹⁴ Bunting and Stefanidis,¹⁴ like Keeffe *et al.*,¹⁹ chose to consider these substituents as deviating, and took as normal the behaviour of disubstituted compounds such as $m\text{-NO}_2$, $p\text{-Cl}$ and $m,m'\text{-(NO}_2)_2$. A major reason advanced for

the deviation of the p -NO₂ substituent was the requirement for extensive solvent reorganization for the nitro group in the enolate ion product relative to the benzyl ketone reactant. The late solvation of the nitro group along the RC will, according to the principle of non-perfect synchronization, lower the intrinsic rate constant. However, it is not clear how water, in the case of ketones, and Me₂SO, in the case of arylnitromethanes, can have comparable solvational effects, when water is known to be most effective in solvating carbanions that have their negative charge largely localized on oxygen atoms, whereas the polarizable Me₂SO efficiently solvates benzene rings.²¹

We believe that the deviations of p -CN- and p -NO₂-substituted aromatic carbon acids are intrinsic to these groups, and may be related to enhanced effective reactants and products force constants. Such force constants can be originated by the participation of CN or NO₂ bonds in the RC, and lead to higher reaction energy barriers. Bunting and Stefanidis¹⁴ observed negative deviations of the p -OCH₃-substituted ketones in the Brønsted plots. Our analysis does not reveal such deviations, which means that the low rate constants observed for methoxy substituted ketones are simply caused by the very negative R value of this substituent.

Stefanidis and Bunting⁶⁰ also studied a series of 4-phenacylpyridines and three series of 4-phenacylpyridinium cations (V–VIII). The essential



feature that distinguishes the structure of these ketones from the previous ones is the separation of the ring substituent from the acidic carbon by the carbonyl group. The distance from the substituent to the leaving proton is now so large that field/inductive and resonance effects may become negligible and no significant variations of n^{\ddagger} within each series are expected. Under these circumstances, η must remain constant in each series. In fact, the average η and the population standard deviation for the series V–VIII are $\eta_{av} = 0.19763$, $\sigma = 0.00030$; $\eta_{av} = 0.19437$, $\sigma = 0.00030$; $\eta_{av} = 0.19487$, $\sigma = 0.00016$; and $\eta_{av} = 0.19511$, $\sigma = 0.00007$. In their analysis, Stefanidis and Bunting⁶⁰ remarked that the methylation of 3- and

4-(X-phenylacetyl)pyridines leads to a lower reactivity, whereas methylation of V leads to an enhanced reactivity. According to our study, the methylation of the first two ketones does not significantly affect their n^{\ddagger} values, as seen from entries p -XPhCH₂COPy_m vs p -XPhCH₂COPy_{Me_m} and p -XPhCH₂COPy_p vs p -XPhCH₂COPy_{Me_p} in Table 11. This means that their intrinsic reactivities are indistinguishable. On the other hand, η_{av} for V is lower than that for VI, indicating an increase in intrinsic reactivity. This is understandable given the strong F effect introduced by the positive charge in the aromatic ring directly attached to the acidic carbon.

The deprotonation of phenylnitromethane by carboxylate anions in Me₂SO–water (90:10) provides a critical test for the validity of the assumption of a negligible (ΔG^0)² effect on η . The high content of Me₂SO in the solvent favours a lower λ and enhances this effect. On the other hand, the substitution in the carboxylate is isolated from the protonation site by a CO group, which was seen to attenuate strongly the electronic effects in the case of aromatic ketones. From the slope of the plot in Figure 6 we obtain $\lambda = 116 \text{ kJ mol}^{-1}$, and from the intercept we extract $n^{\ddagger} = 0.856$. In view of the typical variations of λ with the Me₂SO content of the solvent, we could expect $\lambda > 250 \text{ kJ mol}^{-1}$ for a methanol–water (50:50) solvent mixture. A critical case where a λ value of this size could influence η is the

deprotonation of G'G''CHNO₂ in methanol–water. Calculating n^{\ddagger} under the assumption that $\lambda = 250 \text{ kJ mol}^{-1}$ leads to a poorer correlation of n^{\ddagger} and F and R . This indicates that the actual λ value must be appreciably larger.

The fluorene/fluorenyl system presents a relatively low correlation coefficient. The reaction rates were measured in diethyl ether, and large λ values can be expected. However, the ΔG^0 values involved are close to zero, and will not lead to important corrections. Two other factors may be relevant to the analysis of this system: the polarizability of the alkyl groups and tunnelling. It is well known that alkyl substituents have a very important polarizability effect in the gas phase.⁵⁰

This is completely attenuated in aqueous solution, and even in Me₂SO the charge dispersion by the solvent is efficient. However, in diethyl ether the polarizability of alkyl groups may play a role in the deprotonation rates. Fluorene/fluorenyl proton exchange in diethyl ether is especially suitable for tunnelling. The aromatic rings and the solvent will not contribute appreciably to the RC because of their small distortion in the course of reaction, so the reduced mass of the system can be determined simply from the CH oscillators in reactants and products. However, symmetric systems should have specially favourable tunnelling rates because of resonance,⁶¹ and this is not apparent from the experimental rates. Tunnelling also tends to increase n^* ,²⁸ but the calculated n^* values do not appear to be especially enhanced. Hence we believe that polarizability is the relevant factor not accounted for by our analysis. Actually, the linear correlation between n^* and the polarizability parameters proposed by Taft *et al.*⁵⁷ for gas-phase substituent acidity effects has an appreciable coefficient, 0.92. This system seems to be more sensitive to field/inductive effects than the nitroalkanes. We suggest that the energetic proximity between the HOMO and the LUMO of toluene as compared with nitromethane (Figure 2) is the source of the sensitivity of the TS of fluorenes to electronic perturbation.

Finally, the deprotonation of carbon acids XCH₂X by water also has a modest correlation coefficient. This is easily understandable given the diversity of structures and reactions energies involved. Actually, it is a major achievement of this model to be able to rationalize the behaviour of such diverse species. Acetylacetone has a specially large positive deviation when the force constants described in the Results section are used in the calculations. They neglect the participation of the CO group in the RC. When such participation is considered, using the criteria described for the NO₂ group, the force constants became $f_t = 584$ and $f_p = 608 \text{ J mol}^{-1} \text{ pm}^{-2}$ and $l = 239 \text{ pm}$. The deviation is now strongly negative. This is a good indication that the actual participation of the CO group in the ketone deprotonation RC is smaller than in the case of the NO₂ group in the nitroalkane deprotonation, but that it is significant. We believe that this kind of oversimplification of the RC, which considered the participation of the group adjacent to the acidic carbon only in the case of nitromethane, is one of the main reasons for the modest correlation of the n^* values of this series of carbon acids with field/inductive and resonance effects.

Our analysis has some aspects in common with the treatment by Kresge,⁶ namely in the interpretation of anomalous Brønsted coefficients in terms of intrinsic effects of the substituents on the TS. It differs in the inclusion of resonance effects, which are dominant in some systems, and in the quantitative approach to the deprotonation of carbon acids in general.

The *ad hoc* criteria used to reduce the multi-

dimensionality of the real system may be criticized as a weakness of the model. On the contrary, we believe that the application of the model provides a physically meaningful, tractable, reaction coordinate, involving just enough parameters to account for the effects present in the real systems. Evidence in favour of the progress variable elected for this study comes from the values of n^* lower than 0.5, obtained when the participation of the NO₂ group in the RC is neglected. The model predicts $n^* < 0.5$ for the deprotonation, in water, of carbon acids of the type XCH₂X, when $0.038F + 0.662R < 0.4$. This means that the deprotonations of species such as CH₂(SO₃)₂²⁻ or CH₂(OCOCH₃)₂ in water are not likely to be observed.

CONCLUSION

The application of Formosinho's intersecting-state model to deprotonations of nitroalkanes provides a framework to understand how the nitro group is involved in the reaction coordinate and what effects it causes. The predominant configuration of the carbanion locates the negative charge in the oxygen atoms of the nitro group, leading to appreciable changes in the force constants and bond lengths of this group. As a result, extensive bond reorganization must take place in the course of the reaction. ISM translates this as large force constants for the reactive modes, which lead to relatively slow rates of proton transfer. The high electron affinity provided by the nitro group induces far-reaching consequences to the reactivity of nitroalkanes. The electronic configuration of the transition state becomes very sensitive to the effect of substituents located close to the acid carbon, and may respond more effectively to the small electronic changes they induce than to the free energy for reaction. The outcome may be Brønsted relationships where electronic effects overlap with genuine free energy relationships. Most often, the first effect reinforces the second, and α values larger than unity are observed. This is reflected in Figure 5, given the difference in slopes between the theoretical data calculated with a constant n^* and the experimental series of reactions. Occasionally, the electronic effect dominates and opposes the free energy variation, as in the series CH₃NO₂, CH₂(CH₃)NO₂, CH(CH₃)₂NO₂, and $\alpha < 0$ results. When the electronic and free energy changes influence the rates to comparable extents but opposing each other, curved Brønsted plots may be observed, as in the deprotonation of aryl nitromethanes by benzoate anion in Me₂SO. When the substitution takes place in the base catalyst and the nitroalkane is maintained along a reaction series, the electronic effects are strongly attenuated whereas the free energy changes are large, and 'normal' Brønsted coefficients β can be observed.

The application of ISM to the deprotonation of

ketones and fluorenes reveals the same effects as in the case of nitroalkanes. When other carbon acids are considered, such as $\text{CH}_2(\text{CH}_3\text{CH}_2\text{CO}_2)_2$, $\text{CH}_2(\text{CH}_3\text{CH}_2\text{SO}_2)_2$ and $\text{CH}_2(\text{CN})_2$, the model brings into focus the existence of a mechanistic continuum in the deprotonation of all these acids. The common denominator to all these proton transfers is the change in the transition-state electronic configuration with the ability of the substituents to stabilize a negative charge in the acidic carbon atom.

The present application of the intersecting-state model together with its application to other proton transfers reactions and acid-base catalysis, both in the ground³²⁻³⁴ and excited states,^{35,36} offers a new, wide, window over the field of free energy relationships. This model gives a clear picture of the success and limitations of LFER. Where limitations to LFER occur, ISM may still be applied to probe relative energies of transition states and gain some insight into the corresponding structures. This treatment has the advantage of being more general and of having a deeper physical meaning than LFER, while maintaining a similar simplicity of application.

ACKNOWLEDGEMENT

This work was supported by the Instituto Nacional de Investigação Científica.

REFERENCES

- J. E. Leffler, *Science*, **117**, 340 (1953).
- G. S. Hammond, *J. Am. Chem. Soc.* **77**, 334 (1955).
- A. J. Kresge, *Chem. Soc. Rev.* **2**, 475 (1973).
- F. G. Bordwell, W. J. Boyle, Jr, J. A. Hautala and K. C. Yee, *J. Am. Chem. Soc.* **91**, 4002 (1969).
- F. G. Bordwell, J. E. Bartmess and J. A. Hautala, *J. Org. Chem.* **43**, 3107 (1978).
- A. J. Kresge, *Can. J. Chem.* **52**, 1897 (1974).
- C. F. Bernasconi and P. Paschalis, *J. Am. Chem. Soc.* **111**, 5893 (1989).
- J. R. Murdoch, J. A. Bryson, D. F. McMillen and J. I. Brauman, *J. Am. Chem. Soc.* **104**, 600 (1982).
- F. G. Bordwell and W. J. Boyle, Jr, *J. Am. Chem. Soc.* **94**, 3907 (1972).
- F. Hibbert, in *Comprehensive Chemical Kinetics*, edited by C. H. Bamford and C. F. H. Tipper, Vol. 7, pp. 97-196. Elsevier, Amsterdam (1977).
- R. A. Marcus, *J. Am. Chem. Soc.* **91**, 7224 (1969).
- M. C. Rose and J. Stuehr, *J. Am. Chem. Soc.* **93**, 4350 (1971).
- J. C. Wilson, I. Källsson and W. H. Saunders, Jr, *J. Am. Chem. Soc.* **102**, 4780 (1980).
- J. W. Bunting and D. Stefanidis, *J. Am. Chem. Soc.* **110**, 4008 (1988).
- A. Pross and S. S. Shaik, *J. Am. Chem. Soc.* **104**, 1129 (1982).
- H. Yamataka and S. Nagase, *J. Org. Chem.* **53**, 3232 (1988).
- E. Grunwald, *J. Am. Chem. Soc.* **107**, 125 (1985).
- W. J. Albery, C. F. Bernasconi and A. J. Kresge, *J. Phys. Org. Chem.* **1**, 29 (1988).
- J. R. Keeffe, J. Morey, C. A. Palmer and J. C. Lee, *J. Am. Chem. Soc.* **101**, 1295 (1979).
- N. Agmon, *J. Am. Chem. Soc.* **102**, 2164 (1980).
- C. F. Bernasconi and R. D. Bunnell, *J. Am. Chem. Soc.* **110**, 2900 (1988).
- C. F. Bernasconi, *Tetrahedron*, **42**, 3219 (1985).
- C. F. Bernasconi, D. A. V. Kliner, A. S. Mullin and J. X. Ni, *J. Org. Chem.* **53**, 3342 (1988).
- J. L. Kurz, *J. Am. Chem. Soc.* **111**, 8631 (1989).
- J. W. Bunting and D. Stefanidis, *J. Am. Chem. Soc.* **111**, 5834 (1989).
- D. Stefanidis and J. W. Bunting, *J. Am. Chem. Soc.* **113**, 991 (1991).
- A. J. C. Varandas and S. J. Formosinho, *J. Chem. Soc., Faraday Trans. 2* **82**, 953 (1986).
- S. J. Formosinho, in *Theoretical and Computational Models for Organic Reactions*, edited by S. J. Formosinho, I. G. Csizmadia and L. G. Arnaut, p. 159. Kluwer, Amsterdam (1991).
- H. S. Johnston and C. Parr, *J. Am. Chem. Soc.* **85**, 2544 (1963).
- (a) A. J. C. Varandas, F. B. Brown, C. A. Mead, D. G. Truhlar and N. C. Blais, *J. Chem. Phys.* **86**, 6258 (1987); (b) G. C. Lynch, R. Steckler, D. W. Schwenke, A. J. C. Varandas, D. G. Truhlar and B. C. Garrett, *J. Chem. Phys.* **94**, 7136 (1991).
- G. W. Koeppel and A. J. Kresge, *J. Chem. Soc., Chem. Commun.* 371 (1973).
- L. G. Arnaut and S. J. Formosinho, *J. Phys. Org. Chem.* **3**, 95 (1990).
- S. J. Formosinho, *J. Chem. Soc., Perkin Trans. 2*, 61 (1987).
- S. J. Formosinho and V. M. S. Gil, *J. Chem. Soc., Perkin Trans. 2*, 1655 (1987).
- L. G. Arnaut and S. J. Formosinho, *J. Phys. Chem.* **92**, 685 (1988).
- K. Yates, *J. Phys. Org. Chem.* **2**, 300 (1989).
- S. J. Formosinho, *Tetrahedron*, **42**, 4557 (1986).
- C. Trinquocoste, M. R. Lafon and M.-T. Forel, *Spectrochim. Acta, Part A*, **30**, 813 (1974).
- A. J. Gordon and R. A. Ford, *The Chemist's Companion*, pp. 107, 114. Wiley, New York (1972).
- M. J. S. Dewar, *J. Am. Chem. Soc.* **106**, 209 (1984).
- R. B. Woodward and R. Hoffmann, *Angew. Chem., Int. Ed. Engl.* **8**, 781 (1969).
- R. D. Harcourt, *Qualitative Valence-Bond Descriptions of Electron-Rich Molecules: Pauling '3-Electron Bonds' and 'Increased-Valence' Theory*, Springer, Berlin (1982).
- A. Pross, *Adv. Phys. Org. Chem.* **21**, 99 (1985).
- N. Agmon and R. D. Levine, *J. Chem. Phys.* **71**, 3034 (1979).
- B. C. Garrett, D. G. Truhlar and A. W. Magnuson, *J. Chem. Phys.* **76**, 2321 (1982).
- G. Lendvay, *J. Phys. Chem.* **93**, 4422 (1989).
- D. K. Maity and S. P. Bhattacharyya, *J. Am. Chem. Soc.* **112**, 3223 (1990).
- Z. Shi and R. J. Boyd, *J. Am. Chem. Soc.* **113**, 1072 (1991).
- E. K. Fukuda and R. T. McIver, *J. Phys. Chem.* **87**, 2997 (1983); E. P. Grimsrud, G. Caldwell, S. Chowdhury and P. Kebarle, *J. Am. Chem. Soc.* **107**, 4627 (1985).

50. R. W. Taft, J. L. M. Abboud, F. Anvia, M. Berthelot, M. Fujio, J.-F. Gal, A. D. Headley, W. G. Henderson, I. Koppel, J.-H. Qian, M. Mishima, M. Taagepera and S. Ueji, *J. Am. Chem. Soc.* **110**, 1797 (1988).
51. P. Kebarle and S. Chowdhury, *Chem. Rev.* **87**, 513 (1987).
52. R. Popielarz and D. R. Arnold, *J. Am. Chem. Soc.* **112**, 3068 (1990).
53. R. W. Taft and R. D. Topsom, *Prog. Phys. Org. Chem.* **16**, 1 (1987).
54. C. G. Swain and E. C. Lupton, Jr, *J. Am. Chem. Soc.* **90**, 4328 (1968).
55. C. G. Swain, S. H. Unger, N. R. Rosenquist and M. S. Swain, *J. Am. Chem. Soc.* **105**, 492 (1983).
56. J.-L. M. Abboud, J. Catalán, J. Elguero and R. W. Taft, *J. Org. Chem.* **53**, 1137 (1988).
57. R. W. Taft, I. A. Koppel, R. D. Topsom and F. Anvia, *J. Am. Chem. Soc.* **112**, 2047 (1990).
58. L. Pauling, *J. Am. Chem. Soc.* **69**, 542 (1947).
59. A. R. Katritzky and R. D. Topson, *J. Chem. Educ.* **48**, 427 (1971); J. A. Pople and M. Gordon, *J. Am. Chem. Soc.* **89**, 4253 (1967).
60. D. Stefanidis and J. W. Bunting, *J. Am. Chem. Soc.* **112**, 3163 (1990).
61. R. P. Bell, *The Tunnel Effect in Chemistry*, p. 49. Chapman and Hall, London (1980)
62. V. I. Vedenev, L. V. Gurvich, V. N. Kondrat'yev and Y. L. Frankevich (Eds), *Bond Energies, Ionization Potentials and Electron Affinities*, Arnold, London (1966).
63. E. Lindholm and J. Li, *J. Phys. Chem.* **92**, 1731 (1988); R. G. Pearson, *J. Am. Chem. Soc.* **108**, 6109 (1986); N. Heinrich, W. Koch and G. Frenking, *Chem. Phys. Lett.* **124**, 20 (1986); K. D. Jordan, J. A. Michejda and P. D. Burrow, *J. Am. Chem. Soc.* **98**, 1295 (1976).
64. F. G. Bordwell, W. J. Boyle, Jr, and K. C. Yee, *J. Am. Chem. Soc.* **92**, 5926 (1970).
65. D. J. Barnes and R. P. Bell, *Proc. R. Soc. London, Ser. A* **318**, 421 (1970).
66. R. P. Bell and R. L. Tranter, *Proc. R. Soc. London, Ser. A* **337**, 517 (1974).
67. J. P. Gurthrie, *Can. J. Chem.* **57**, 1177 (1979).
68. R. P. Bell, G. R. Hillier, J. W. Mansfield and D. G. Street, *J. Chem. Soc. B* 827 (1967).
69. R. G. Pearson and R. L. Dillon, *J. Am. Chem. Soc.* **75**, 2439 (1953).